Performance of Powder-Injection-Molded W-4.9Ni-2.1Fe Components

Y.S. Zu, Y.H. Chiou, and S.T. Lin

A 93 wt% W heavy alloy was injection molded into standard tensile test specimens and kinetic energy penetrators. Due to the relatively high activation energy of flow (124 kJ/mol), the rheological behavior of the molten feedstock was very susceptible to temperature variation. Using die sets with constant-volume die cavities, the tensile test specimens could be formed within a wide working window, whereas the penetrator could not be molded without defects because of different jetting phenomena during molding. The penetrator could be molded successfully using a die set whose die cavity progressively expanded during molding. The parts thus formed could subsequently be processed into intact components with full density and low carbon contents (<100 ppm). Their mechanical properties were comparable to or better than those of conventionally processed tungsten heavy alloys. Additional penetration test results indicated that powder injection molding was a viable route for processing high-performance tungsten heavy alloys.

Keywords

kinetic energy penetrator, mechanical properties, powder injection molding, rheological behavior, tungsten heavy alloy

1. Introduction

TUNGSTEN heavy alloys are a class of two-phase composite materials processed by liquid-phase sintering of mixed elemental powders. Their microstructures are characterized by spheroidal tungsten grains embedded in a ductile matrix phase. Typical compositions of tungsten heavy alloys include W-Ni-Fe, W-Ni-Cu, W-Ni-Fe-Co, and W-Co-Ni, with W-Ni-Fe having been studied intensively and shown to have superior mechanical properties (Ref 1-3).

Heavy alloys based on the composition of W-Ni-Fe usually contain 80 to 98 wt% W and an optimal nickel-to-iron ratio of 7:3 as the rest (Ref 1, 4). Due to their unique combination of high hardness (50 to 70 HRA), high strength (ultimate tensile strength, 800 to 1100 MPa), high ductility (tensile elongation, 10 to 35%), and high density (16 to 18 g/cm^3), tungsten heavy alloys are usually utilized as kinetic energy penetrators, armor, shaped charge liners, and inertial counterweight balances (Ref 1, 5-7). Most of these applications require complex final configurations. However, because of high hardness and toughness of tungsten heavy alloys, extensive tool wear usually results during machining. Thus, net-shape or near-net-shape fabrication routes such as injection molding provide a cost-effective alternative.

Powder injection molding (PIM) is a powder processing route that combines several of the process characteristics of powder metallurgy and plastic injection molding (Ref 8). It is capable of mass producing monolithic or composite materials into components with intricate geometries. It has substantially replaced other competitive processes in the fabrication of metallic and ceramic components, especially for materials that are difficult to cast or machine. In this process, a suitable powder is mixed with an appropriate amount of binder. The mixture is then injection molded into a green body. A debinding step at which binder is removed without deteriorating the composition and shape of the component is carefully controlled before the powder compact is sintered to a high final density.

Several prior studies on the injection molding of tungsten heavy alloys showed that it was possible to achieve properties comparable to those obtained by conventional press-and-sintered tungsten heavy alloys (Ref 9-11). Nevertheless, only specimens with simple geometries were investigated, and processing defects could still be observed. For successful PIM, attention must be focused on all sequential processing steps, because defects formed at each step cannot be cured in later steps. Consequently, this research was carried out to investigate the possibility of fabricating kinetic energy penetrators by PIM. The factors affecting the success of this process were also examined.

2. Experimental Procedures

The heavy alloy used in this study was 93W-4.9Ni-2.1Fe (weight percent). The characteristics of the powders are listed in Table 1. The powders were blended and milled in a plastic jar for 24 h using type 304 stainless steel balls. The binder was composed of polypropylene (PP, 20 wt%), ethylene vinyl acetate (EVA, 25 wt%), paraffin wax (PW, 50 wt%), and stearic acid (SA, 5 wt%), the melting temperatures of which were 169, 92, 70, and 59 °C, respectively. The milled powder and binder

Table 1 Characteristics of the starting powders

Characteristic	Powder		
	Tungsten	Nickel	Iron
Vendor	Korea Tungsten	Novamet	BASF
Grade	KM-8	INCO 4SP	OM
Average particle size, μm	3	10	4
Tap density, g/cm^3	5.8	4.7	4.3
Major impurities, wt%	O, 0.08	C, 0.05	N, 0.90
		O, 0.02	C, 0.89
		Fe, 0.01	O, 0.30
		S, 0.001	

Y.S. Zu, Y.H. Chiou, and **S.T. Lin,** Mechanical Engineering Department, National Taiwan Institute of Technology, Taipei, Taiwan, Republic of China.

were blended at 180 °C for about 80 min, using a Z-blade mixer. The volume fraction of powder loading was 0.5

Standard tensile test specimens (Ref 12) and kinetic energy penetrators were injection molded using a reciprocating-screw injection-molding machine. The tensile test specimen had a maximum length of 100 mm and a minimum diameter of 5 mm in the gage section; the kinetic energy penetrator had a maximum length of 56.5 mm and a maximum diameter of 15.2 mm. Two different die sets were used to mold the kinetic energy penetrator. The first die set had a fixed-volume die cavity. The other had a progressively expanding die cavity (Ref 13).

The injection-molded parts were subjected to a two-stage debinding treatment that comprised a sequential combination of solvent extraction and thermal debinding (Ref 14). Such an approach can dramatically reduce the debinding time and avoid possible shape distortion, contamination of wicking powder, and formation of internal voids. The debinding parameters were optimized using the statistical results of an experimental matrix based on the Taguchi method (Ref 15).

During solvent extraction, the parts were immersed in heptane, which was maintained at 55 °C. The extraction times for the tensile test specimens and kinetic energy penetrators were 8 and 24 h, respectively. Thermal debinding was conducted in a tube furnace using a protective atmosphere of dry hydrogen. The thermal profile was as follows: heating at a rate of 5 K/min to 300 °C, holding for 1 h, followed by additional heating at a rate of 3 K/min to 550 °C, holding for 2 h.

Sintering was carried out immediately following the isothermal holding at 550 °C. The sintering schedule involved heating at a rate of 10 K/min to the sintering temperature of either 1480, 1500, or 1520 °C, then holding for either 20, 40, or 60 min. Dry hydrogen was also used in sintering until the last 10 min of the isothermal hold, when the atmosphere was changed to dry argon to avoid hydrogen embrittlement (Ref 16).

The rheological behavior of the molten feedstock was examined by capillary extrusion, using a capillary 2 mm in diameter and 41 mm long. Sintered density was measured by the water immersion method. Ultimate tensile strength was determined at a crosshead speed of 1 mm/min, where the true stress at fracture was reported. Tensile elongation was normalized with respect to a gage length of 25.4 mm. Hardness was tested using a Rockwell hardness tester on the A scale. The residual carbon content was determined by combustion method (Leco 2023, Leco Corp., St. Joseph, MI).

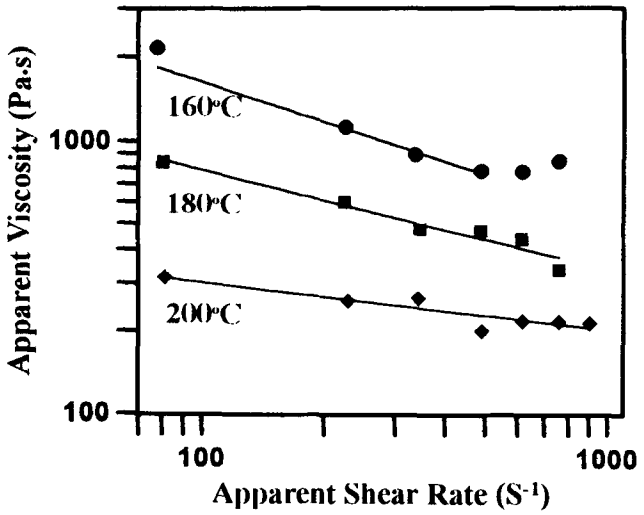

Fig. 1 Variation of apparent viscosity of the molten feedstock with apparent shear rate and test temperature

3. Results and Discussion

3.1 *Rheological Behavior*

For lack of a better approach, the rheological behavior of a particulate-filled polymer is usually expressed in terms of apparent shear stress (τ) and apparent shear rate ($\dot{\gamma}$) through the power law (Ref 17):

$$\tau = K\dot{\gamma}^n \quad \text{(Eq 1)}$$

where K and n are respectively defined as fluid consistency index and flow behavior index. A fluid behaves in a manner of pseudoplastic flow, Newtonian flow, or dilatant flow when its flow behavior index is smaller than, equal to, or greater than 1, respectively. Apparent viscosity (η) is defined as the ratio of apparent shear stress to apparent shear rate:

$$\eta = \frac{\tau}{\dot{\gamma}} = K\dot{\gamma}^{n-1} = K_0 e^{E/RT}\dot{\gamma}^{n-1} \quad \text{(Eq 2)}$$

where K_0 is an empirical constant coefficient, E is the activation energy flow, R is the universal gas constant, and T is the absolute temperature.

Figure 1 shows the relationship between apparent viscosity and apparent shear rate for the feedstock tested at different temperatures. The molten feedstock exhibited psuedoplastic flow behavior in the temperature and strain-rate ranges investigated, except for dilatant flow behavior at a test temperature of 160 °C and for shear rates greater than 500/s. Such a tendency was due to insufficient activation of the binder components during testing, because the test temperature was lower than the melting temperature of polypropylene (169 °C). The flow behavior indexes (n) for the molten feedstock were 0.52, 0.63, and 0.83 for test temperatures of 160, 180, and 200 °C, respectively. Thus, the molten feedstock gradually transformed from a psuedoplastic fluid into a Newtonian-like fluid as the test temperature increased. A molten feedstock exhibiting Newtonian flow behavior is ideal for injection molding, because the melt viscosity can be maintained constant over a wide range of shear rates, and superplastic deformation behavior may be achieved (Ref 18). Although a high test temperature was preferred from the viewpoint of rheological behavior, vaporization of binder components was very severe, which impedes packing of the molten feedstock during molding.

Figure 2 shows the temperature dependency of apparent viscosity in the form of an Arrhenius expression. In the temperature range of interest, the activation energy of flow was 124 kJ/mol. Such a value was much higher than 3.2 kJ/mol for a zirconia feedstock exhibiting superplastic behavior (Ref 18), or

about 20 kJ/mol for most injection-moldable feedstocks (Ref 19). Thus, the rheological behavior of the feedstock was very susceptible to temperature variation, and a slight decrease in melt temperature could result in a large increase in melt viscosity. Such a trend was detrimental to the success of molding if the feedstock cooled rapidly in the die cavity.

The unfavorable rheological behavior of the feedstock was caused by use of a tungsten powder with a mean particle size of 3 μm. Conventional processes such as uniaxial die pressing usually use tungsten powders with a mean particle size range of 3 to 5 μm (Ref 1, 6, 7, 16). On the other hand, tungsten powders with mean particle sizes of 3 μm (Ref 11) and 10 μm (Ref 9) are used for powder injection molding. In this study, the fine tungsten powder was selected in order to avoid possible exudation of binder from powder during injection molding and to minimize slumping of the parts during debinding. Additionally, direct comparison with the conventionally processed tungsten heavy alloys could be made.

Because tungsten has a relatively high density compared with the binder components, it is possible that the binder might exude from the powder in the molding stage and that shape distortion caused by gravity force might occur in the debinding stage. Exudation of binder from powder, which is caused by insufficient interfacial cohesion, causes severe abrasion against the injection molding machine and results in nonuniform density in green molded parts. To minimize exudation of binder, interfacial cohesion between the tungsten powder and the binder should be improved, and the lubrication mechanism of particles could be shifted from boundary lubrication to fluid lubrication (Ref 20). Such a transition was achieved by using a fine powder and by increasing binder viscosity. Both factors in turn enhanced the green strength of the as-molded parts and reduced the tendency of the part to slump during debinding. However, the rheological behavior of the feedstock deteriorated as the critical powder loading of the feedstock was reduced (Ref 8).

3.2 *Injection Molding*

High-density parts with excellent properties were made under a wide range of injection molding conditions. Typical conditions are summarized in Table 2. Note the relatively high die temperature and the long packing and cooling times. The specimens could be molded at lower die temperatures, but obvious cold-weld interfaces were found.

It was difficult to successfully mold the kinetic energy penetrator using the die set having a constant-volume die cavity. Since the cross-sectional area variation from gate into die cavity was very large, different jetting phenomena occurred during molding. Entrapped pores were found in the specimens when the injection molding speed and the melt temperature were high—a consequence of conventional jetting (Ref 21). The entrapped pores could not be squeezed out, even when vents were introduced, and higher packing pressures and longer packing times were employed.

Table 2 Typical injection molding conditions for the standard tensile test specimen

Temperature, °C	Time, s	Pressure, MPa
Rear barrel, 170	Injection, 5	First injection, 4
Middle barrel, 180	Packing, 20	Second injection, 5
Front barrel, 185	Cooling, 75	Final injection, 8
Die, 80		Packing, 6

At lower injection speeds and lower melt temperatures, void-free compacts could be molded. However, severe cold-weld interfaces existed in the compacts. When these compacts were exposed to solvent during the solvent extraction stage, relaxation of the residual stresses near the cold-weld interfaces resulted in springlike compacts (Fig. 3). This observation indicated that solid-state jetting had taken place during molding (Ref 21), a result of the high activation energy of flow of the molten feedstock.

A new die set with a progressively expanding die cavity (Ref 13) was tested. Figure 4 schematically describes the filling pattern of this die set. During molding, the die cavity constantly expanded along the symmetrical axis of the penetrator until completely filled. Thus, the newly formed section of the die cavity could be completely filled with the hot melt under high

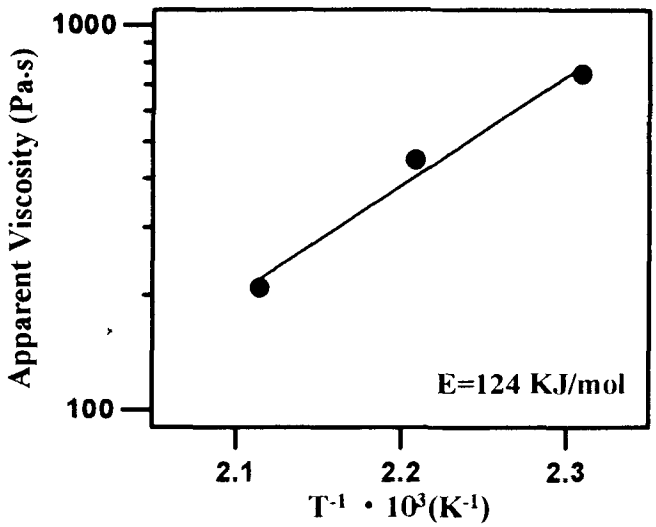

Fig. 2 Temperature dependency of apparent viscosity in the form of an Arrhenius expression

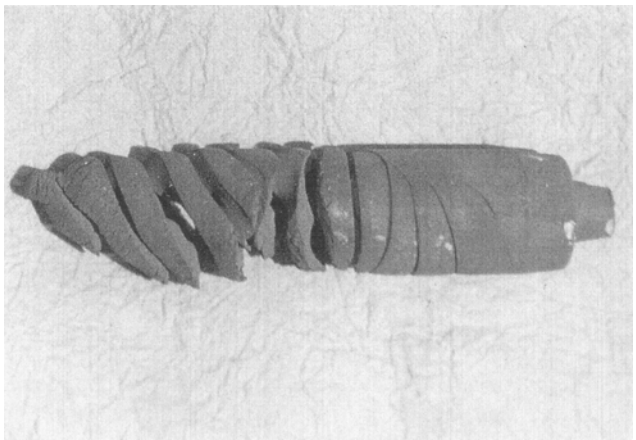

Fig. 3 Formation of a springlike green part when the as-molded penetrator was immersed in heptane at a temperature of 55 °C. Length, ~600 mm

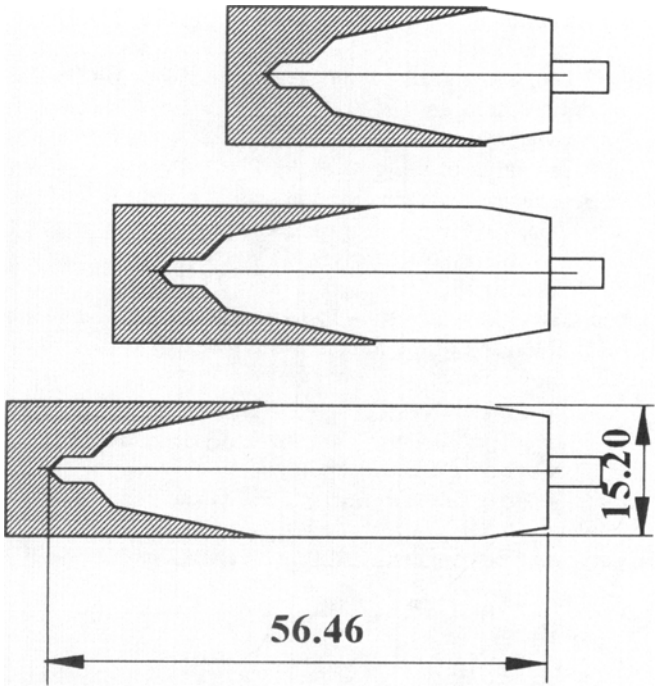

Fig. 4 Filling pattern of the penetrator for a die set with a progressively expanding die cavity. Dimensions given in millimeters.

Table 3 Mechanical properties of tungsten heavy alloys processed by different approaches

Tungsten content, wt%	Ultimate tensile strength, MPa	Elongation, %	Hardness, HRA	Process, conditions	Ref
90	1090	21	68	Swaged, heat treated	25
93	960	25	64	As sintered	24
93	950	10	...	As sintered	7
93	1050	30	...	As sintered	26
93	1000	21	...	Heat treated	7
93	1120	8	70	Swaged	6
93	930	30	63	PIM, as sintered	11
93	1100	25	64	PIM, as sintered	(a)
95	950	20	50	PIM, heat treated	9

(a) Present work

pressures. This type of filling pattern was like extruding the molten feedstock in a closed-end die set in that jetting was avoided. Void-free compacts could be successfully molded and subsequently processed into defect-free penetrators.

3.3 *Sintered Properties*

Figures 5 and 6 illustrate the effects of sintering temperature and isothermal holding time at 1500 °C, respectively, on the concentration of tungsten atoms in the matrix phase, average grain size, contiguity of tungsten phase, hardness, ultimate tensile strength, and tensile elongation. Both enhanced sintering temperature and prolonged isothermal holding time at 1500 °C

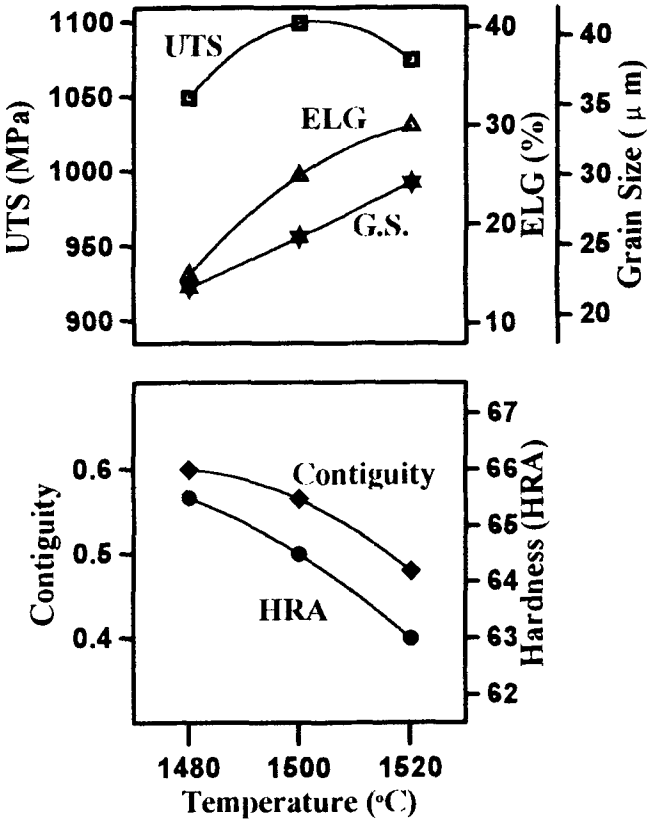

Fig. 5 Effect of sintering temperature on average tungsten grain size, contiguity of tungsten grains, hardness, ultimate tensile strength, and tensile elongation. Isothermal holding time, 40 min

resulted in decreased contiguity of tungsten grains and hardness of the alloy, due to the repartitioning of tungsten atoms from the matrix phase toward the tungsten grains (Ref 22). A low contiguity of tungsten grains was preferred because fracture along the tungsten grain boundaries usually accompanied low ductility (Ref 23). The average tungsten grain size and tensile elongation increased with increased sintering temperature and sintering time, while the ultimate tensile strength exhibited the highest value at a sintering temperature of 1500 °C and an isothermal holding time of 40 min. Decreasing the contiguity of tungsten grains while still constraining the average tungsten grain size under 20 μm improved the toughness of tungsten heavy alloys.

Subsequent to sintering at 1500 °C for 40 min, the average sintered shrinkage ratio was 22.6% and sintered density was 17.9 g/cm^3. Because the matrix phase was a solid solution composed of nickel, iron, and different dissolved concentrations of tungsten, calculation of the theoretical density of the alloy was impossible. Thus, the theoretical density achieved by the PIM process could only be estimated by microstructural examination. Figure 7 shows the microstructure of a specimen that experienced a tensile elongation of 23%. Clearly, the specimen was processed too close to full density. In addition, extensive tensile elongation was achieved prior to the nucleation of a crack, which can be observed from the elongated tungsten grains.

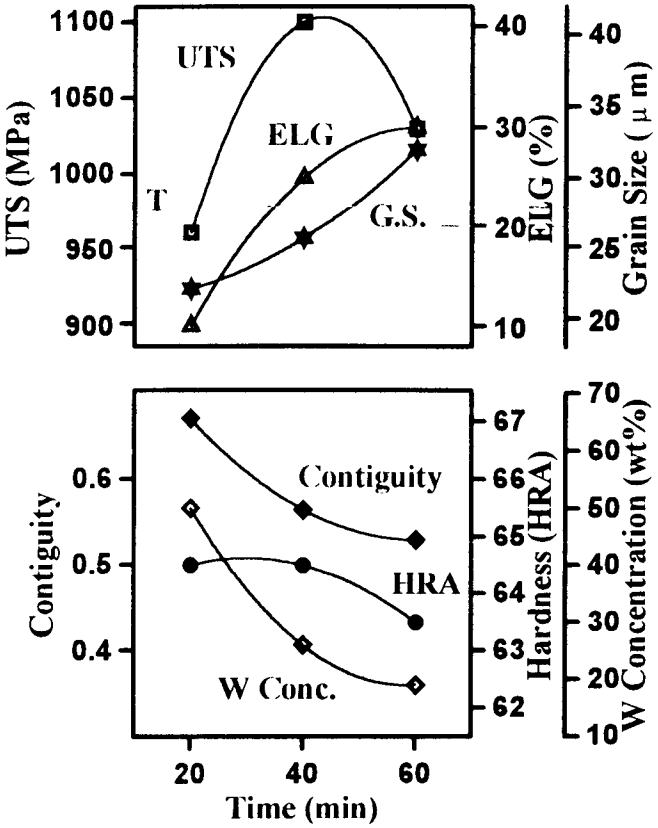

Fig. 6 Effect of isothermal holding time at a sintering temperature of 1500 °C on dissolved concentration of tungsten atoms in the matrix phase, average tungsten grain size, contiguity of tungsten grains, hardness, ultimate tensile strength, and tensile elongation

The mechanical properties of conventionally processed (Ref 6, 7, 24-26) and injection-molded (Ref 9, 11) tungsten heavy alloys are compared in Table 3. Commercial tungsten heavy alloys are usually heat treated, or swaged and heat treated, to improve their mechanical properties. Heat treatment of tungsten heavy alloys is usually carried out by a fast cooling from about 1200 °C to avoid the precipitation of brittle phases (Ref 3, 4, 9). Swaging is usually performed to remove possible defects, such as pores and segregation of matrix phase (Ref 6, 7, 25), and is usually followed by a heat treatment to relieve the stress associated with deformation during swaging. Caution must be exercised when comparing the strength and ductility values shown in Table 3, because almost no detail was given in the cited literature with respect to cross-sectional area and gage length. However, it is apparent that the mechanical properties achieved in this study were comparable to or even better than those cited in the literature.

Figure 8 shows the effect of residual carbon content on the ultimate tensile strength and tensile elongation of the heavy alloy. These data were collected from the results of an experimental matrix where the debinding conditions were varied (Ref 15). Although the correlation is weak, an identifiable trend of decreasing ductility and increasing strength with increasing residual carbon content can be seen. The residual carbon content was controlled to levels lower than the suggested criterion of

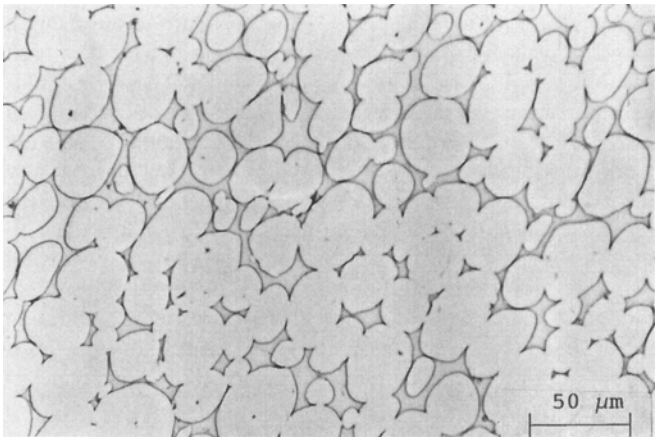

Fig. 7 Microstructure of a 93 wt% W heavy alloy that experienced 23% tensile elongation

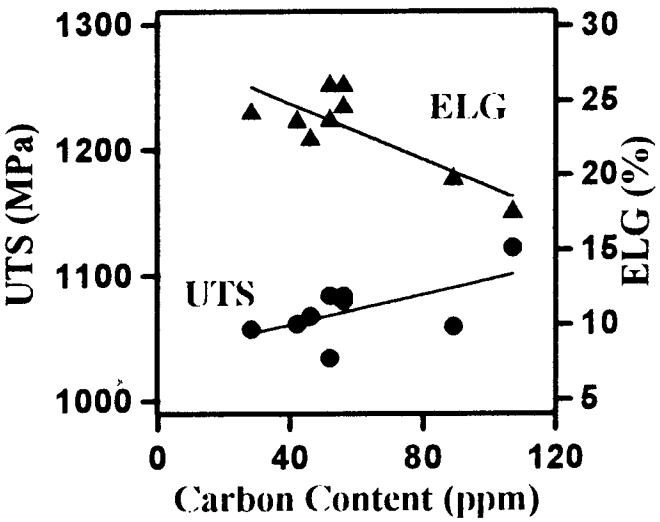

Fig. 8 Correlation of ultimate tensile strength and tensile elongation with residual carbon content

100 ppm, above which precipitation of brittle η carbide near the interface between a tungsten grain and the matrix phase was suggested (Ref 27). In fact, a residual carbon content greater than 60 ppm was found to be detrimental to the toughness of this heavy alloy (Ref 15).

A standard penetration test was conducted for the assembled kinetic energy penetrators. The penetrators were launched from a 20 mm smooth-bore gun at an initial velocity of 1030 m/s. The target, a heat-treated SAE 4130 steel plate with a thickness of 35 mm and a hardness of 42 HRC, was located 200 m from the gun. Ten penetrators were fired. They were able to penetrate the steel plate with good firing precision; the randomly distributed penetrated holes in the steel plate could be circled to a minimum diameter of 185 mm.

4. Conclusions

To avoid the possible exudation of binder from powder during molding and slumping of parts during debinding, injection

molding of a 93 wt% W heavy alloy was carried out using a tungsten powder with a mean particle size of 3 μm and a high fraction of polymeric materials in the binder. These two unfavorable factors caused the rheological behavior of the molten feedstock to be susceptible to temperature variation. Thus, the working window for injection molding was very narrow, and the kinetic energy penetrators could be successfully molded only by using a die set with a progressively expanding die cavity. The molded compacts were debound by a two-stage solvent debinding approach and sintered at 1500 °C for 40 min to yield products with excellent mechanical properties. Penetration tests proved that injection molding was satisfactory for fabricating high-performance tungsten heavy alloy kinetic energy penetrators.

References

1. D.J. Jones and P. Munnery, Production of Tungsten Alloy Penetration Radiation Shields, *Powder Metall.*, Vol 10, 1967, p 156-173
2. W.E. Gurwell, A Review of Embrittlement Mechanisms in Tungsten Heavy Alloys, *Prog. in Powder Metallurgy*, Vol 42, E.A. Carlson and G. Gaines, Ed., Metal Powder Industries Federation, 1986, p 569-590
3. B.C. Muddle, Interphase Boundary Precipitation in Liquid Phase Sintered W-Ni-Fe and W-Ni-Cu Alloys, *Metall. Trans. A*, Vol 15A, 1984, p 1089-1098
4. D.V. Edmonds and P.N. Jones, Interfacial Embrittlement in Liquid-Phase Sintered Tungsten Heavy Alloys, *Metall. Trans. A*, Vol 10A, 1979, p 289-295
5. W.D. Schubert, Aspects of Research and Development in Tungsten and Tungsten Alloys, *Refract. Met. Hard Mater.*, Vol 11, 1992, p 151-157
6. T.W. Penrice, Development in Materials for Use as Kinetic Energy Penetrators, *Powder Metallurgy in Defense Technology*, Vol 5, Metal Powder Industries Federation, 1980, p 11-21
7. D. Chaiat, Future P/M Materials for Kinetic Energy Penetrators and Shape Charge Liners, *Powder Metallurgy in Defense Technology*, Vol 7, W.J. Ullrich, Ed., Metal Powder Industries Federation, 1987, p 185-197
8. R.M. German, *Powder Injection Molding*, Metal Powder Industries Federation, 1990, p 1-16
9. A. Bose, R.J. Dowding, and G.A. Allen, Powder Injection Molding of a 95W-4Ni-1Fe Alloy, *Powder Injection Molding Symposium—1992*, P.H. Booker, J. Gaspervich, and R.M. German, Ed., Metal Powder Industries Federation, 1992, p 261-274
10. A. Bose, H. Zhang, P. Kemp, and R.M. German, Injection Molding of Molybdenum Treated Tungsten Heavy Alloys, *Advances in Powder Metallurgy*, Vol 3, E.R. Andreotti and P.J. McGeehan, Ed., Metal Powder Industries Federation, 1990, p 401-413
11. T.S. Wei and R.M. German, Injection Molded Tungsten Heavy Alloy, *Int. J. Powder Metall.*, Vol 24, 1988, p 327-335
12. S.T. Lin and R.M. German, Properties of Fully Densified Injection Molded Carbonyl Iron, *Metall. Trans. A*, Vol 21A, 1990, p 2531-2538
13. G.C. Sih, Progressively Expanding Molding with Single or Multiple Selection Controlling Volume Configuration and Rate of Injection Material: Metal or Polymer, U.S. Patent 5,505,896, 1996
14. S.T. Lin and R.M. German, Extraction Debinding of Injection Molded Parts by Condensed Solvent, *Powder Metall. Int.*, Vol 21, 1989, p 19-24
15. Y.S. Zu and S.T. Lin, "Optimizing the Mechanical Properties of Injection Molded W-4.9%Ni-2.1%Fe in Debinding," National Taiwan Institute of Technology, Taipei, 1996
16. A. Bose and R.M. German, Sintering Atmosphere Effects on Tensile Properties of Heavy Alloys, *Metall. Trans. A*, Vol 19A, 1988, p 2467-2476
17. D.J. Williams, *Polymer Science and Engineering*, Prentice-Hall, 1972, p 340-355
18. Y.H. Chiou, S.J. Liu, and S.T. Lin, Superplastic Behaviour of a Zirconia Powder-Binder Blend, *Ceram. Int.*, Vol 22, 1996, p 35-41
19. P.H. Booker, "Particulate Injection Molding of Selected Metal Alloys and Ceramics," presented at 1991 Injection Molding International Symposium (Albany), Metal Powder Industries Federation, 15-17 July 1991
20. R.M. German, K.F. Hens, and S.T. Lin, Key Issues in Powder Injection Molding, *Bull. Am. Ceram. Soc.*, Vol 70, 1991, p 1294-1302
21. N. Piccirillo and D. Lee, Jetting Phenomena in Powder Injection Molding, *Int. J. Powder Metall.*, Vol 28, 1992, p 13-25
22. Y.H. Chiou, Y.S. Zu, and S.T. Lin, Partition of Tungsten in the Matrix Phase for Liquid Phase Sintered 93%W-4.9%Ni-2.1%Fe., *Scr. Mater.*, Vol 34, 1996, p 135-140
23. R.M. German, J.E. Hanafee, and S.L. Digiallonardo, Toughness Variation Test Temperature and Cooling Rate for Liquid Phase Sintered W-3.5Ni-1.5Fe, *Metall. Trans. A*, Vol 15A, 1984, p 121-128
24. R.M. German and L.L. Bourguignon, Analysis of High Tungsten Content Heavy Alloys, *Powder Metallurgy in Defense Technology*, Vol 6, C.L. Freeby and W.J. Ullrich, Ed., Metal Powder Industries Federation, 1985, p 117-131
25. J.M. Sakai and C. Grabarek, Ballistic Tests on Heat Treated Tungsten Alloy Penetrator after Swaging, *Powder Metallurgy in Defense Technology*, Vol 4, Metal Powder Industries Federation, 1978, p 85-90
26. L.L. Bourguignon and R.M. German, Sintering Temperature Effects on Tungsten Heavy Alloys, *Int. J. Powder Metall.*, Vol 24, 1988, p 115-121
27. J.B. Posthill, M.C. Hogwood, and D.V. Edmonds, Precipitation at Tungsten/Tungsten Interfaces in Tungsten-Nickel-Iron Heavy Alloys, *Powder Metall.*, Vol 29, 1986, p 45-51